Coherency Enforcement in the Cluster of Heterogeneous Grid-forming and Grid-following Inverters

Muhammad F. Umar, Amirhosein Gohari Nazari, Mohammad B. Shadmand Dept. of Electrical & Computer Engineering, University of Illinois Chicago, IL, USA mumar6@uic.edu, agohar2@uic.edu, shadmand@uic.edu

Abstract— This paper presents a control scheme for enforcing coherency in a power electronics dominated grid (PEDG) comprising multiple grid-forming (GFM) and grid-following inverters (GFL) based distributed generation (DG). Based on different applications and grid requirements, the primary control for DG can vary such as GFM, GFL, etc. Moreover, each DG can have unique parameters such as controller gains, power ratings, and filter model parameters. All these factors intrinsically contribute towards the heterogeneity in the PEDG. Furthermore, DGs are increasing steeply to integrate renewable energy generation. Therefore, performing different analysis on such a large network is becoming a big challenge recently. One of the solutions is performing aggregation based on similar behaving DGs that can significantly decrease the computational burden and analysis time. Thus, this paper proposes coherency enforced (CE) control to acquire coherent and homogeneous dynamic characteristics for inherently heterogenous cluster of GFM and GFL inverters based DGs. Various case studies are presented to validate the effectiveness of the proposed approach.

Keywords— coherency in generation sources, heterogenous cluster, emulation of virtual inertia, homogeneity in dynamic response.

I. INTRODUCTION

The existing power grid is being modified to include abundance of renewable energy sources (RES) such as solar-PV and wind energy. By the end of 2023, globally installed capacity of the solar energy will reach total of 440 GW out of which 159 GWs of rooftop solar-PV will be installed [1]. Moreover, the global installed capacity for the wind energy at the end of 2023 will be 892 GWs [2]. Unlike the conventional power grid where most of the generation was centralized and based on synchronous generators (SG). Considering such enormous amount of renewable energy, the structure of existing power system moves from centralized generation to distributed generation (DG). This would be realized through several RES integrated to the grid via power electronic interface such as, inverters. Therefore, this will lead to a new energy paradigm known as power electronics dominated grid (PEDG) [3, 4]. Generally, the inverters in PEDG are controlled as grid following (GFL) or grid-forming (GFM) modes. PEDG offers several advantages such as fast acting generation via GFL based DG to support the transient stability of the power grid [5, 6], safe islanded operation via GFM based DG [7, 8], and other auxiliary services are provided to the power grid with mix of GFL and GFM based DG in cluster [9].

Although PEDG has several favorable features for a promising candidate to incorporate the renewable energy, the considerable rise of the number of generation units in the PEDG intensifies the complexity of the grid [10]. Moreover, the dynamic behavior of each DG in PEDG depends upon various factors such as type of control scheme, filter parameters, controller gains, etc. Thus, the electromagnetic transient model of PEDG will comprise various dynamical states spanning over numerous timescales. So, modeling the PEDG for stability assessment and resiliency with huge number of DGs is a big challenge. The complexity of the network can be solved via accurate aggregate models and reduced order model of PEDG [11]. However, the intrinsic heterogeneity in DGs is present due to different control schemes i.e., GFL or GFM, filter model parameters, network impedances, and power ratings. Therefore, the dynamic response of each DGs to the disturbances in PEDG would be different and conclusively most of the DGs in PEDG are non-coherent. Resultantly devising the precise reduced or insightful aggregated model of the PEDG and minimizing the complexity is a challenging task.

Traditionally, in the conventional power systems, a coherency-based aggregation modelling is utilized to obtain the reduced-order model of multiple coherent SGs that makes the economic and optimized dispatching faster [12]. In more details, the coherency among the generation sources in the network is claimed for which the frequency or voltage angle dynamics are similar to a disturbance [13, 14]. As the core of the generation units changes from SGs to power electronic converters, the coherency-based aggregation concept in power system can be reconstructed to be used for the PEDG [15, 16]. In the current literature few works have reported to develop the coherency identification and enforcement schemes but still this area of research has gap and haven't been addressed comprehensively. The work in [17] leverages the concept of differential geometry and apply it to cluster of inverters to identify the coherent group of inverters in the given cluster. However, the analysis was performed considering smaller cluster and extending the proposed scheme to higher order network requires extensive analysis and validation. For the virtual synchronous generator (VSG) based modular multilevel inverters (MMI) the coherency based equivalence method is proposed in [18]. Specifically, the power angles of similar behaving MMIs are used to group the coherent group of inverters. However, limited accuracy of the developed

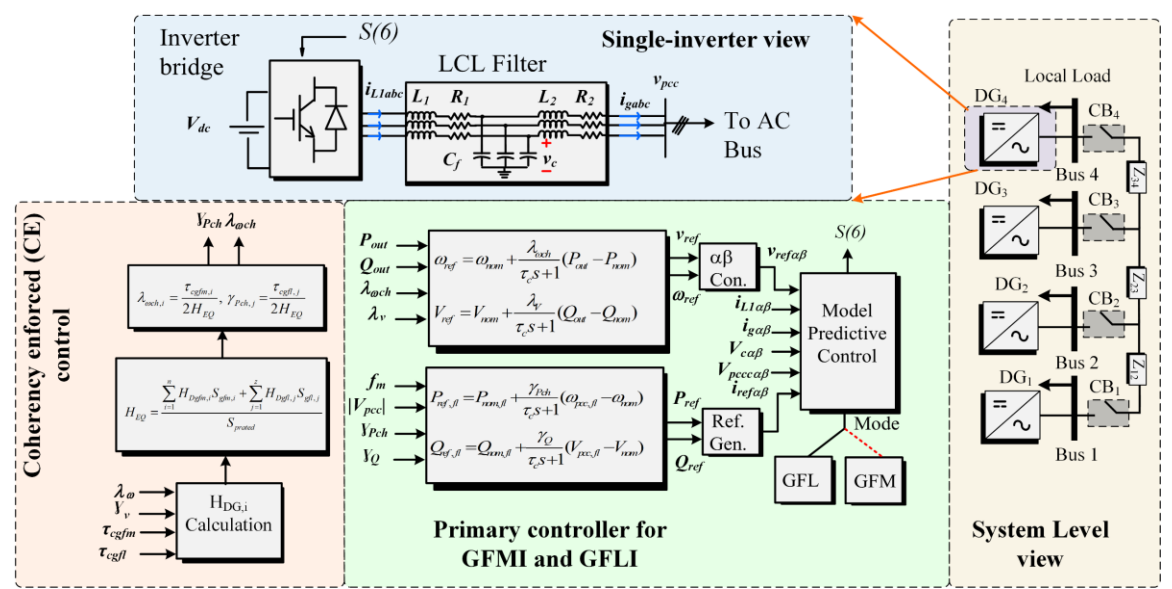


Fig. 1. Understudy system with structure of proposed coherency enforced (CE) control and the primary controller for GFM and GFL based DGs in PEDG.

equivalence method is reported. Another work in [19], reports the use of virtual impedance method to force the coherency in the cluster of droop-controlled inverters. Then, eigenvaluebased perturbation scheme is utilized to identify the coherent dynamics of the droop-controlled inverters. Nevertheless, the proposed scheme in [19], considers all DGs have similar physical parameter and can't be generalized on the intrinsically heterogenous cluster of inverters. Moreover, only voltagecontrolled inverters are considered in the previous works, but the future of the power grid will contain mix of voltage control and current controlled inverters, i.e., GFM and GFL based DGs. Therefore, still a generalized scheme to enforce the coherency among the heterogenous cluster of inverters is still missing in the previous literature.

Thus, this work presents a coherency enforced (CE) control built on autonomously calculating the equivalent inertia of the cluster based on the primary controller's parameters of the DGs in PEDG. Then, adjusting each DGs inertia coefficient such as they exhibit similar dynamics under various grid disturbances. Therefore, this will diminish the heterogeneous dynamic behavior and enforce coherency in the PEDG comprising GFL and GFM control based DGs. Moreover, this will provide a necessary step before the clustering of multiple DGs and enables its insightful aggregated model. Remainder of work the work is structured as; the description of the PEDG and its related primary controllers is given in section II. The mathematical modelling and algorithm explanation of the proposed CE control is presented in section II. The section IV provides simulation-based validation of the proposed CE control and comparison without the proposed control. In the section V the work is concluded with some remarks and future works.

II. DESCRIPTION OF SYSTEM UNDERSTUDY

The understudy heterogenous PEDG is comprised of four DGs as depicted in the Fig. 1. The intrinsic heterogeneity in the PEDG is introduced due to different controllers, filter parameters and power ratings. DG1 and DG2 has GFM control and DG₃ and DG₄ primary are controlled in GFL mode to inject active and reactive power in the grid. The other system parameters associated with the PEDG is given in the Table I. The voltage reference generated from GFM mode of DG and current reference for the GFL mode are regulated via a dualmode model predictive control scheme. The mode is selected based on the type of the reference given to the MPC block. Mode 1 refers to the voltage control mode and mode 2 is denoted as the current control mode of the dual-mode MPC block. More granular details about the primary controllers in the PEDG are provided in the succeeding subsections.

A. Grid forming control of DG

The GFM mode of operation refers as the controlled AC voltage source behind the coupling impedance. For the DGs that are controlled in the GFM mode, the frequency reference and voltage magnitude reference are given by,

$$\omega_{ref} = \omega_{nom} + \frac{\lambda_{\omega}}{\tau_{c}s + 1} (P_{out} - P_{nom,fm})$$
 (1)

$$V_{ref} = V_{nom} + \frac{\lambda_{V}}{\tau_{c} s + 1} (Q_{out} - Q_{nom, fm})$$
 (2)

where the ω_{nom} and V_{nom} are the nominal value of angular frequency and voltage, ω_{ref} and V_{ref} are reference values of the angular frequency and magnitude of the output voltage. By using (1) and (2) the voltage reference is generated and then transformed to stationary reference frame to devise the $\vec{v}_{ref,\alpha\beta}$. Furthermore, $P_{nom,fm}$ and $Q_{nom,fm}$ are the nominal active and reactive power that the GFM based DG injects to the grid. τ_c is the time constant of the low-pass filter. The λ_{ω} and λ_{ν} are referred as the controller gains and calculated by,

$$\lambda_{\omega} = \frac{\omega_{\min,fm} - \omega_{\max,fm}}{P_{\max,fm} - P_{\min,fm}} \tag{3}$$

$$\lambda_{\omega} = \frac{\omega_{\min,fm} - \omega_{\max,fm}}{P_{\max,fm} - P_{\min,fm}}$$

$$\lambda_{V} = \frac{V_{\min,fm} - V_{\max,fm}}{Q_{\max,fm} - Q_{\min,fm}}$$
(3)

where, $\omega_{min,fm}$ and $\omega_{max,fm}$ are the minimum and maximum values of the allowable frequency range, $P_{min,fm}$ and $P_{max,fm}$ are the minimum and maximum active power injection capability which is based on the rating of the DG. $V_{min,fm}$ and $V_{max,fm}$ are the minimum and maximum allowable voltage magnitude range. $Q_{min,fm}$ and $Q_{max,fm}$ are the minimum and maximum value of the reactive power and it is dependent upon the DG's reactive power ratings. The generated reference PCC voltage (v_{ref}) is converted to the stationary reference frame and then fed to the model predictive control (MPC) block to regulate the PCC voltage of the GFM based DGs.

B. Grid-following control of DG

The GFL control of the DGs is based on the frequency-watt regulation. In this method, the commanded active and reactive power are injected to the grid. This active and reactive power references have two parts; (i) value of active and reacted power injected during steady-state conditions, and (ii) active and reactive power injected during the transients to support the grid. Thus, the active and reactive power references are calculated by,

$$P_{ref} = P_{nom,fl} + \frac{\gamma_P}{\tau_c s + 1} (\omega_{PCC,fl} - \omega_{nom})$$
 (5)

$$Q_{ref} = Q_{nom,fl} + \frac{\gamma_Q}{\tau_c s + 1} (V_{PCC,fl} - V_{nom})$$
 (6)

where $\omega_{PCC,fl}$ and $V_{PCC,fl}$ are the angular frequency and magnitude of the PCC voltage of the grid following inverter. $P_{nom,fl}$ and $Q_{nom,fl}$ are the active and reactive power that the GFL DG injects to the grid when the frequency of its PCC voltage is nominal. The controller's gains are given by,

$$\gamma_P = \frac{P_{\text{max},fl} - P_{\text{min},fl}}{\omega_{\text{min},fl} - \omega_{\text{max},fl}} \tag{7}$$

$$\gamma_Q = \frac{Q_{\text{max},fl} - Q_{\text{min},fl}}{V_{\text{max},fl} - V_{\text{min},fl}}$$
(8)

based on the (5) and (6), the output current reference in dq reference frame is given as,

$$i_{dref} = \frac{P_{ref} v_{pccd} + Q_{ref} v_{pccq}}{v_{pccd}^2 + v_{pccq}^2}$$
(9)

$$i_{qref} = \frac{P_{ref} v_{qccd} - Q_{ref} v_{pccq}}{v_{pccd}^2 + v_{pccq}^2}$$
(10)

then, the output current reference in stationary reference frame based on (9) and (10) is given by,

$$\begin{bmatrix} i_{\alpha ref} \\ i_{\beta ref} \end{bmatrix} = \begin{bmatrix} \cos \theta_{pcc} - \sin \theta_{pcc} \\ \sin \theta_{pcc} & \cos \theta_{pcc} \end{bmatrix} \begin{bmatrix} i_{dref} \\ i_{qref} \end{bmatrix}$$
(11)

$$i_{\text{vof }\alpha\theta} = i_{\text{vof }\alpha} + ji_{\text{vof }\theta} \tag{12}$$

where, θ_{pcc} refers to the common ac bus voltage angle. This output current reference in the stationary reference frame is then fed as an input to the MPC block to project the optimized switching pulses to the inverter's bridge.

C. Dual-mode model predictive control scheme

The MPC scheme is based on predicting the one step ahead states of the given circuit model and then minimizing the cost

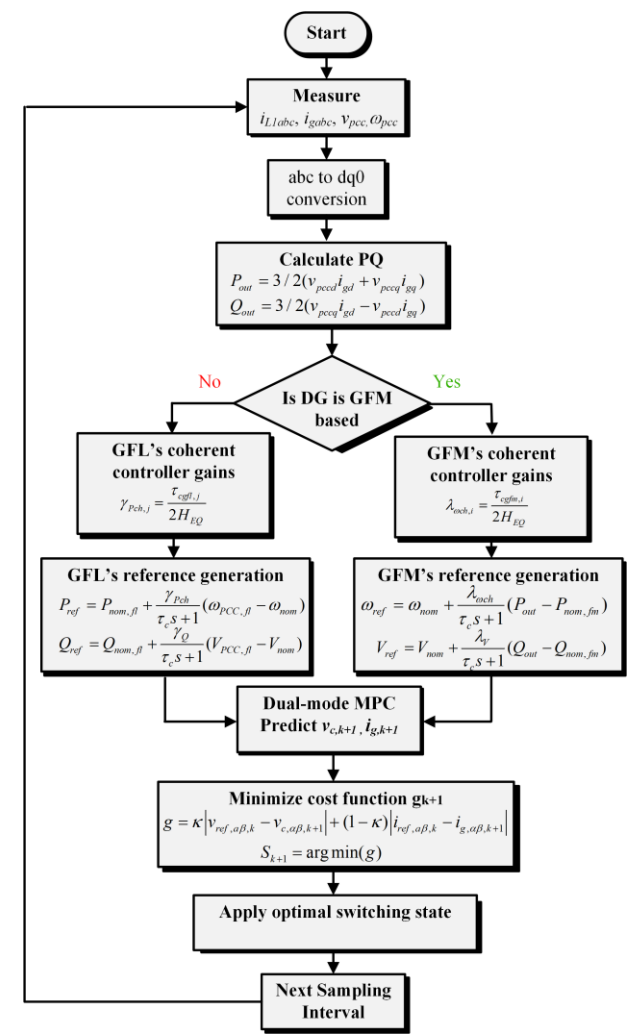


Fig. 2. Algorithm flowchart of the proposed CE control

function devised to compare the predicted state and reference. For the scope of this work, the inverter bridge is interfaced with the LCL filter. More details about the modeling and the prediction of the controllable state variables are given in [7, 20]. Thus, the dual mode cost function subjected for minimization is provided as,

$$g = \kappa \left| v_{ref,a\beta,k} - v_{c,\alpha\beta,k+1} \right| + (1 - \kappa) \left| i_{ref,a\beta,k} - i_{g,\alpha\beta,k+1} \right|$$

$$S_{k+1} = \arg \min(g)$$
(13)

where κ refers to the controller action constant. Specifically, if the κ has value of one, then GFM mode of MPC is selected and when κ is equal to zero, the MPC acts in current controlled mode. $v_{c,\alpha\beta,k+l}$ is the one-step ahead predicted capacitor voltage, and $i_{g,\alpha\beta,k+l}$ is the one-step ahead predicted output current. This step ahead capacitor voltage and output current are predicted by using the state-space model of three phase inverter interfaced with LCL filter.

III. PROPOSED COHERENCY ENFORCED (CE) CONTROL

Fig. 1 illustrates the structure of the proposed CE control. Because of the similarities between the dynamics of swing equation of the synchronous generator and droop-based control of DGs, the relation of inertia emulation from the DGs in PEDG can be derived [21]. Thus, the inertia constant of individual

DGs operating with droop and reverse-droop control is given by,

$$H_{Dgfm} = \frac{\tau_{cgfm}}{2\lambda_{\omega}}, \quad H_{Dgfl} = \frac{\tau_{cgfl}}{2\gamma_{P}}$$
 (14)

where, H_{Dgfm} and H_{Dgfl} refers to the inertia constant for a GFM based DG and GFL based DG, respectively. Based on each DG's inertia constant, the equivalent inertia constant is calculated by,

$$H_{EQ} = \frac{\sum_{i=1}^{n} H_{Dgfm,i} S_{gfm,i} + \sum_{j=1}^{z} H_{Dgfl,j} S_{gfl,j}}{S_{prated}}$$
(15)

where, n is total number of GFM based DGs and z is total number of GFL based DGs. $S_{gfm,i}$ and $S_{gfl,j}$ refers to the respective nominal powers of GFM and GFL based DGs and S_{prated} is the summation of the rated powers of all DGs in the PEDG. Thus, the controller gains that enforce the coherency among the DGs are then calculated by modifying each DG's inertia according to the equivalent inertia. Thus, the coherent gains are then given by,

$$\lambda_{\omega ch,i} = \frac{\tau_{cgfin,i}}{2H_{EO}}, \, \gamma_{Pch,j} = \frac{\tau_{cgfl,j}}{2H_{EO}}$$
 (16)

where, $\lambda_{\omega ch,i}$ and $\gamma_{pch,j}$ are the coherent gains for the GFM and GFL based DGs, respectively. The detailed algorithm flowchart is illustrated in Fig. 2. The coherency among the cluster of DGs can be established if similar dynamics of voltage angle or frequency are exhibited by the DGs in response to a disturbance. Initially, the voltage, current and frequency measurements are measured and then these measurement signals are converted to $dq\theta$ reference frame. The active and reactive power contribution from each DG is calculated by dq components of the PCC voltage and output current from each DG. Furthermore, based on each DGs' primary controller (GFM or GFL), the respective coherent gains are calculated via (14)-(16). Then, these coherent controller gains are incorporated in the primary controller to generate the current reference for the GFL based DGs and voltage reference for the GFM based DGs. These voltage and current reference are then fed to the dual-mode MPC and then based on the mode of control the value of the k is set to either 0 for the GFL control mode or 1 for the GFM mode of control. The MPC cost function in (13) is minimized to find the optimal switching vector and switching sequence corresponding to that minimized cost function is fed to the three-phase inverter bridge to devise the coherency in the heterogenous PEDG.

IV. SIMULATION RESULTS AND DISCUSSION

The effectiveness of the proposed control is validated for a heterogenous grid cluster consists of interconnected DGs as depicted in the Fig.1. In the cluster DG₁ and DG₂ have a primary control based on GFM while DG₃ and DG₄ are operated based on the GFL control scheme. The considered system's parameters are given in the Table I. It can be noticed from the Table I that the power ratings, LCL filter parameters and the controller's gains have unique values for each DG. Thus, the considered PEDG is intrinsically heterogenous due to dissimilar system parameters.

Table I: System Specifications

Parameter	Value
S_1, S_2, S_3, S_4	11.7, 10.5, 9.4, 8.2 kVA
L_{11} , L_{12} , L_{13} , L_{14}	0.2,0.17,0.14,0.12 mH
L_{21} , L_{22} , L_{23} , L_{24}	3,2.25,2,1.85 μΗ
C_{f1} , C_{f2} , C_{f3} , C_{f4}	75, 69, 63,57 μF
$\lambda_I, \; \lambda_2$	$(3.56, 5.58) \times 10^{-3}$
¥1, ¥2,	$(0.93, 0.45) \times 10^{-3}$

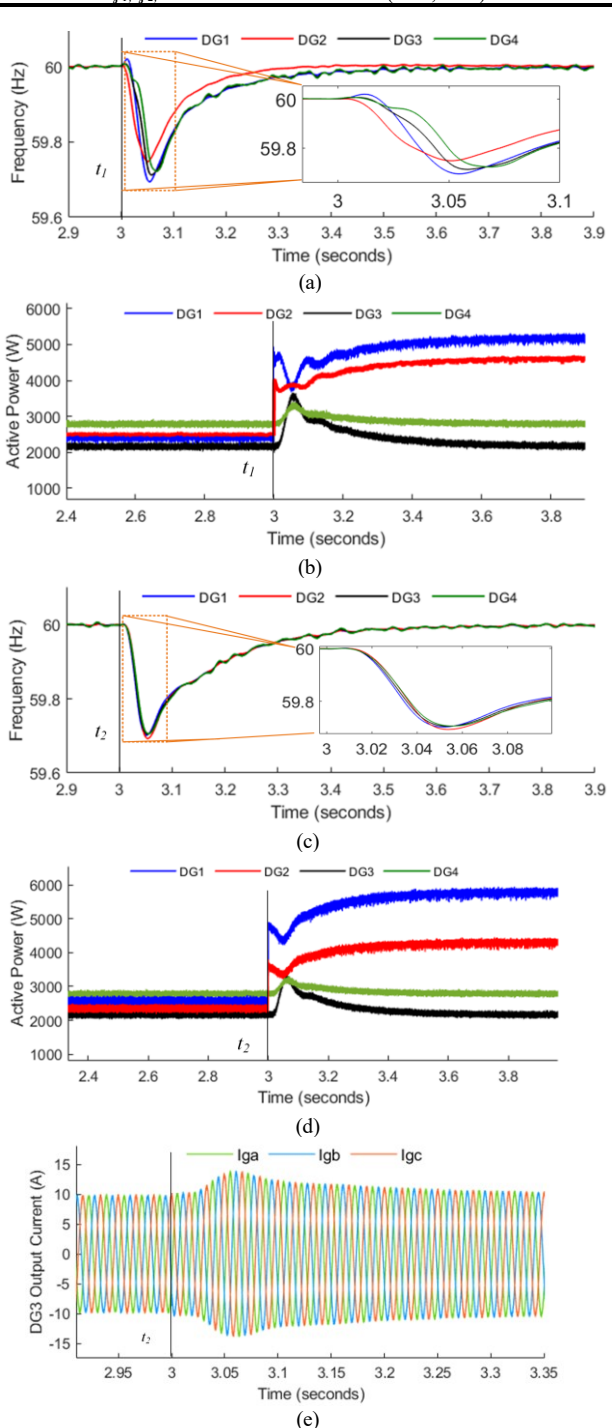


Fig. 3. Case study I: heterogeneous PEDG comprising GFM and GFL based DGs under the transition of step increase in load: (a) frequency of DGs without CE control, (b) Active power profile of DGs without CE, (c) DGs frequency dynamic response with CE, (d) Active power profile with CE, (e) DG₃ output current.

The disturbance in the PEDG is introduced via load step increase and load step decrease at different instances of the time.

A. Case study I: Step increase in load

In this case study, the effect of a step increase in load is observed on heterogenous PEDG that is initially non-coherent and then compared with an enforced coherent PEDG with proposed CE control. Fig. 3 (a) illustrates the dynamics in the frequency during the load disturbance. Specifically, at instant t₁, a step load of 5 kW is added that equates to 50% of the nominal operating point. It can be verified from Fig.3 that all the DGs have different frequency dynamic response and thus, depicts the non-coherent behavior. Furthermore, the active power profile of the noncoherent cluster in response to load change is illustrated in the Fig.3 (b). The active power of the DG₁ and DG₂ changes from 2.4 kW to 5.2 kW and 2.5 kW to 4.6 kW, respectively. Moreover, it is worthy to mention that the GFL based DGs support the system during the transients and injects active power. Therefore, the active power of the DG₃ and DG₄ changes from nominal value of 2.25 kW to 3.6 kW and 2.91 kW to 3.30 kW, respectively during the transient and return to the nominal values in the steady state. The proposed CE control is applied on the heterogenous PEDG, and same step increase in load is added at instant t2 to validate the enforced coherent response. Fig. 3 (c) illustrates the coherent frequency dynamics during the load disturbance with the proposed CE control. Particularly, all the DGs based on GFM and GFL controllers have similar frequency dynamic response to a disturbance and thus, coherency in the heterogenous PEDG is asserted. Fig. 3 (d) depicts the active power profiles of the DGs with the proposed CE control. It can be observed that DG₁ and DG₂ that are based on the GFM control architectures are sharing the amount of load change while DG₃ and DG₄ that have the GFL based control are supporting the grid during the transients and returning to the nominal values during the steady-state conditions. Moreover, the support from the GFL based DGs during the transients is verified from the Fig. 3 (e) that depicts the DG₃ output current. The output current of DG3 increases from the nominal value of 9.5 A_{peak} to 13.5 A_{peak} at instant t_2 and return to it nominal value when the transient stage is over.

B. Casestudy II: Step decrease in load

This case study refers to the condition when a step decrease in the load occurs in the heterogenous PEDG. Specifically, 5 kW of the load is dropped to prove the effectiveness of the proposed CE control in enforcing coherency during the decrement of load. At instant t_3 step decrease of load occurred in the heterogenous PEDG. Fig. 4 (a) illustrates the frequency dynamic response during this disturbance. All the DGs have heterogenous frequency response to the load disturbance and thus, the PEDG is noncoherent. Moreover, the active power profile of the non-coherent PEDG is depicted in Fig. 4 (b). As the load is decreased the active power from the DG₁ and DG₂ is reduced while the DG₃ and DG₄ that are based on GFL reduces their active powers during the transients and return to nominal values after the transient stage is ended. In contrast, with the proposed CE control the coherency is enforced in the heterogenous PEDG and verified by introducing the disturbance. Precisely, at instant t_4 a step decrease of 5 kW is introduced in the system. Fig. 4 (b) shows the dynamic response

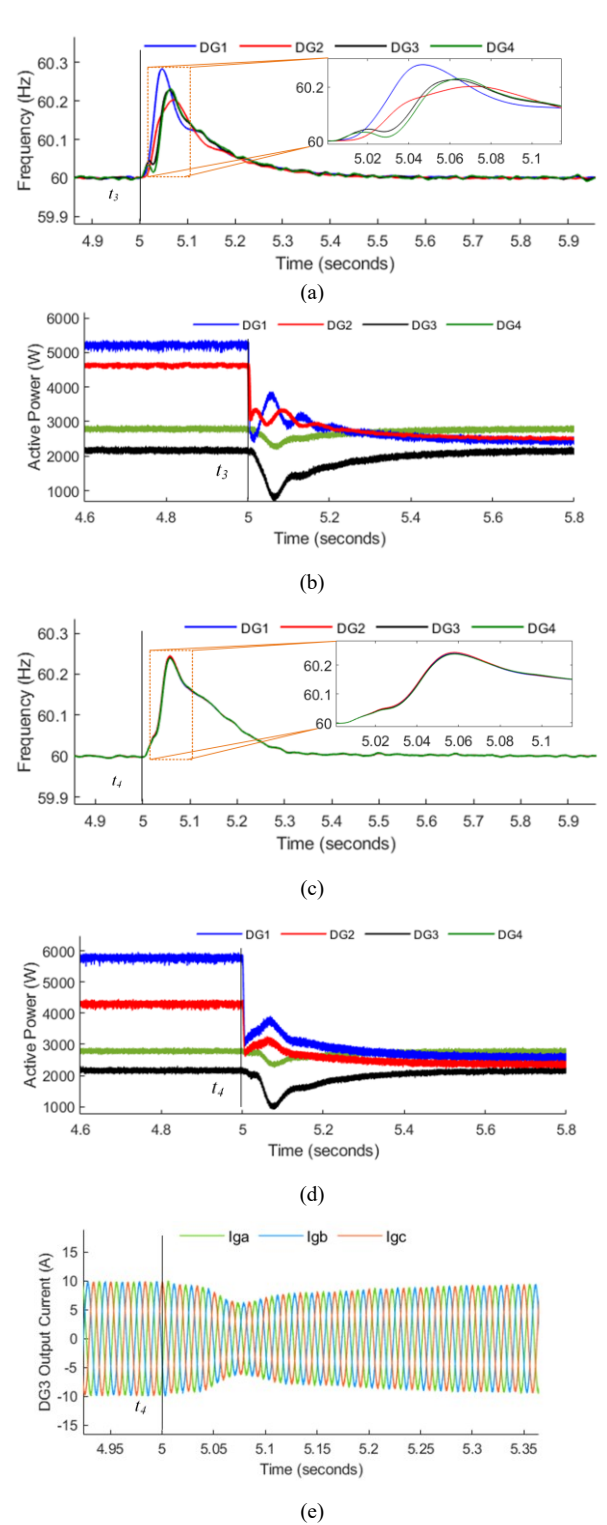


Fig. 4. Case study II: heterogeneous PEDG comprising GFM and GFL based DGs under the transition of step decrease in load: (a) frequency of DGs without CE control, (b) Active power profile of DGs without CE, (c) DGs frequency dynamic response with CE, (d) Active power profile with CE, (e) DG₃ output current.

of the frequency during the disturbance. It is validated during this load disturbance with proposed CE control that all the DGs have similar frequency response and conclusively these are acting in coherent manner. Similarly, the active power profile of coherent

DGs during the transients and steady state are illustrated in the Fig. 4 (d). The active power of the DG_1 and DG_2 is reduced from 5.9 kW to 2.6 kW and 4.44 kW to 2.4 kW, respectively. Moreover, the GFL control based DG_3 and DG_4 reduces their active powers during the transient stage. This can be further verified from the DG_3 output current waveform as depicted in the Fig. 4 (e). The output current of GFL based DG_3 is reduced from 9.5 A_{peak} to 5.5 A_{peak} value to support the system during the transient stage. Thus, based on these two case studies, it is concluded that in any type of load disturbance the heterogenous PEDG with proposed CE control behaves in coherent manner and that can be further used in deriving the insightful aggregated models of the higher order PEDG.

V. CONCLUSION

This paper presented a scheme to enforce coherency in the PEDG consisting multiple heterogenous GFL and GFM based DGs. This coherency among the heterogenous DGs will serve as a necessary step to derive the accurate and insightful aggregated or reduced order model of the large-scale PEDG. The effectiveness of the proposed scheme was verified via introducing a load disturbance and comparing the dynamic frequency response and active power for non-coherent and then forced coherent cluster. The enforced coherent cluster exhibits homogenous frequency dynamic response to the increase and decrease in load disturbance. Thus, by enforcing coherency with proposed control the aggregated model of large-scale PEDG is derived that can make the analysis on the PEDG simpler and computationally efficient.

ACKNOWLEDGMENT

This work was supported by the U.S. National Science Foundation under Grant ECCS-2114442. The statements made herein are solely the responsibility of the author.

REFERENCES

- [1] IEA, "Renewable Energy Market Update June 2023." [Online]. Available: https://www.iea.org/reports/renewable-energy-market-update-june-2023,
- [2] G. W. E. Council, "GWEC Global Wind Report 2019," Global Wind Energy Council: Bonn, Germany, 2017.
- [3] O. H. Abu-Rub, A. Y. Fard, M. F. Umar, M. Hosseinzadehtaher, and M. B. Shadmands, "Towards intelligent power electronics-dominated grid via machine learning techniques," *IEEE Power Electronics Magazine*, vol. 8, no. 1, pp. 28-38, 2021.
- [4] A. Khan, M. Hosseinzadehtaher, M. B. Shadmand, S. Bayhan, and H. Abu-Rub, "On the stability of the power electronics-dominated grid: A new energy paradigm," *IEEE Industrial Electronics Magazine*, vol. 14, no. 4, pp. 65-78, 2020.
- [5] M. Hosseinzadehtaher, A. Zare, A. Khan, M. F. Umar, S. D. silva, and M. B. Shadmand, "AI-based Technique to Enhance Transient Response and Resiliency of Power Electronic Dominated Grids via Grid-Following Inverters," *IEEE Transactions on Industrial Electronics*, pp. 1-11, 2023, doi: 10.1109/TIE.2023.3265067.

- [6] M. F. Umar, A. Khan, and M. B. Shadmand, "A Stabilizer based Predictive Control Scheme for Smart Inverters in Weak Grid," in 2020 IEEE Texas Power and Energy Conference (TPEC), 6-7 Feb. 2020 2020, pp. 1-6, doi: 10.1109/TPEC48276.2020.9042561.
- [7] B. Nun, M. F. Umar, A. Karaki, M. B. Shadmand, S. Bayhan, and H. Abu-Rub, "Rank-Based Predictive Control for Community Microgrids With Dynamic Topology and Multiple Points of Common Coupling," *IEEE Journal of Emerging and Selected Topics in Industrial Electronics*, vol. 3, no. 1, pp. 144-155, 2022, doi: 10.1109/JESTIE.2021.3110746.
- [8] M. F. Umar, M. Hosseinzadehtaher, M. B. Shadmand, H. Livani, and M. Ben-Idris, "A Corrective Scheme to Prevent Adverse Dynamic Interaction of Grid-forming Inverters," in 2023 IEEE Power & Energy Society Innovative Smart Grid Technologies Conference (ISGT), 2023: IEEE, pp. 1-5.
- [9] B. Nun, M. F. Umar, and M. B. Shadmand, "Enabling Resilient Community Microgrids with Multiple Points of Common Coupling via a Rank-Based Model Predictive Control Framework," in 2021 IEEE Applied Power Electronics Conference and Exposition (APEC), 2021: IEEE, pp. 2686-2691.
- [10] Y. Gu, N. Bottrell, and T. C. Green, "Reduced-order models for representing converters in power system studies," *IEEE Transactions on Power Electronics*, vol. 33, no. 4, pp. 3644-3654, 2017.
- [11] O. Ajala, N. Baeckeland, B. Johnson, S. Dhople, and A. Domínguez-García, "Model Reduction and Dynamic Aggregation of Grid-forming Inverter Networks," *IEEE Transactions on Power Systems*, pp. 1-16, 2022, doi: 10.1109/TPWRS.2022.3229970.
- [12] J. H. Chow, R. Galarza, P. Accari, and W. W. Price, "Inertial and slow coherency aggregation algorithms for power system dynamic model reduction," *IEEE Transactions on Power Systems*, vol. 10, no. 2, pp. 680-685, 1995.
- [13] R. Podmore, "Identification of coherent generators for dynamic equivalents," *IEEE Transactions on Power Apparatus and Systems*, no. 4, pp. 1344-1354, 1978.
- [14] X. Wang, V. Vittal, and G. T. Heydt, "Tracing generator coherency indices using the continuation method: A novel approach," *IEEE Transactions on Power Systems*, vol. 20, no. 3, pp. 1510-1518, 2005.
- [15] M. F. Umar, M. Hosseinzadehtaher, and M. B. Shadmand, "Homogeneity realization for cluster of heterogeneous grid-forming inverters," in 2021 6th IEEE Workshop on the Electronic Grid (eGRID), 2021: IEEE, pp. 01-06
- [16] M. F. Umar, M. Hosseinzadehtaher, and M. B. Shadmand, "Enabling Aggregation of Heterogenous Grid-Forming Inverters via Enclaved Homogenization," *IEEE Access*, vol. 10, pp. 94765-94777, 2022.
- [17] X. Du, Y. Zhang, Q. Li, Y. Xiong, X. Yu, and X. Zhang, "New theory of extended coherency for power system based on method of coherency in differential geometry," in 2011 Asia-Pacific Power and Energy Engineering Conference, 2011: IEEE, pp. 1-6.
- [18] C. Li, J. Xu, and C. Zhao, "A coherency-based equivalence method for MMC inverters using virtual synchronous generator control," *IEEE Transactions on Power Delivery*, vol. 31, no. 3, pp. 1369-1378, 2015.
- [19] P. J. Hart, R. H. Lasseter, and T. M. Jahns, "Coherency identification and aggregation in grid-forming droop-controlled inverter networks," *IEEE Transactions on Industry Applications*, vol. 55, no. 3, pp. 2219-2231, 2019.
- [20] M. F. Umar et al., "Single-Phase Grid-Interactive Inverter With Resonance Suppression Based on Adaptive Predictive Control in Weak Grid Condition," *IEEE Journal of Emerging and Selected Topics in Industrial Electronics*, vol. 3, no. 3, pp. 809-820, 2022, doi: 10.1109/JESTIE.2021.3103675.
- [21] J. Liu, Y. Miura, and T. Ise, "Comparison of Dynamic Characteristics Between Virtual Synchronous Generator and Droop Control in Inverter-Based Distributed Generators," *IEEE Transactions on Power Electronics*, vol. 31, no. 5, pp. 3600-3611, 2016, doi: 10.1109/TPEL.2015.2465852.